

**A review on CZTS (Cu<sub>2</sub>ZnSnS<sub>4</sub>) synthesis methods and characterisation**

T. Yahaya, K. I. Mohammed, A. A. Abubakar and K. U. Isah

School of Physical Sciences, Physics Department, Federal University of Technology, Minna,  
Nigeria  
yahayatitus250@gmail.com**Abstract**

*Cu<sub>2</sub>ZnSnS<sub>4</sub>, copper, zinc, tin, sulphide (CZTS) is a p-type semiconductor with high absorption coefficient and a low cost promising absorber material, having a direct band gap from 1 to 1.5 eV, which is ideal for making absorber layer for solar cell. Owing to the cost effective noble metal, less abundance and industrial large scale application purpose, an effective replacement of indium and gallium in CuIn<sub>x</sub>Ga<sub>1-x</sub>S(Se)<sub>2</sub> (CIGS) is highly demanded. There are several approaches to improving the performance of as solar cell by enhancing the power conversion efficiency with a less costly and facile device. In this work we present a brief review on different synthesis methods and characterisation of CZTS material. It is therefore, essential for engineering of CZTS material and the optimisation of the fabrication method for the improvement of solar cell.*

**Keywords--** Cu<sub>2</sub>ZnSnS<sub>4</sub>, Optimisation, Fabrication.

**1.0 INTRODUCTION**

Lately, it is feasible to take the resources and natural elements into accounts because of the emergence of solar cells (Huang *et al.*, 2016). Aside from silicon-based solar cell, the CuIn<sub>x</sub>Ga<sub>1-x</sub>S(Se)<sub>2</sub> (CIGS) thin film solar based cell has drawn in much consideration since its fine steadiness and potential power conversion (Huang *et al.*, 2016). In any case, the use of costly materials like indium and additionally gallium expands the manufacturing. Lately, Cu<sub>2</sub>ZnSnS<sub>4</sub> (CZTS) was seriously examined and expected to be the most encouraging contender to replace Cu(In,Ga)Se<sub>2</sub> (CIGS) (Camara *et al.*, 2013), in which raw materials utilized have minimal expenses, less toxic, and earth abundant. Besides, CZTS likewise has an immediate band gap of 1.4–1.5 eV with high absorption coefficient in the visible ranngge (>10<sup>4</sup> cm<sup>-1</sup>) (Khare *et al.*, 2011).

The Cu<sub>2</sub>ZnSnS<sub>4</sub> (CZTS) compound, non-toxic and abundant, can be a potential alternative for the light absorbing layer in the thin film devices of solar cells to replace conventional absorbent layers, such as CdTe and Cu.In; Ga/Se<sub>2</sub> (CIGS) (Li *et al.*, 2012). Shockley–Queisser balance calculations also show that the photon theoretical limit efficiency of CZTS thin film solar cells is 32.2% (Zhou *et al.*, 2011). CZTS has an absorption coefficient of over 10<sup>4</sup> cm<sup>-1</sup> with band gap of about 1.5 eV (Leitao *et al.*, 2011). It is a semiconductor material of p-type, I2-II-IV-VI4 quaternary compound by substitution of selenium with sulfur, indium with zinc and gallium with tin in the CuInGaSe<sub>2</sub> (CIGS) compound (Mali *et al.*, 2012). Each component of CZTS is easily available and abundant in the Earth's crust: copper (Cu) 50 ppm, zinc (Zn) 75 ppm, tin (Sn) 2.2 ppm and sulfur (S) 260 ppm. These characteristics in combination make it suitable to have exciting findings, ensuring widespread and low cost applications in thin film solar cells. Moreover these properties are the key factors needed to make solar technology competitive with carbon based fuels (Mali *et al.*, 2012).

Therefore, synthesis of CZTS micro- or nanocrystallines has attracted much attention, and then, many solution-based processes have been proposed, such as hot-injection method, hydrothermal method, solvothermal method, and microwaveirradiated method, Sol gel method, Electrospinning (Liu *et al.*, 2013) and several others. Generally, there are two principal crystallographic phase structures of CZTS, which are the so-called stannite (space group I42m) and kesterite (space group I4) (Chen *et al.*, 2009). The only difference between the two structures is the arrangement of Cu

and Zn atoms. It has been experimentally confirmed that CZTS usually crystallizes in kesterite phase as it is thermodynamically more stable than the stannite (Schorr, 2007).

## 2.0 DIFFERENT METHODS OF SYNTHESIS

### 2.1 Electrochemical deposition method

Electrochemical deposition is a coating method to reduce the cations in the aqueous solution, organic solution, or hot-dip fluid in the cathode by supplying potential difference with external circuit power. In the 1970s, people began to try the electrochemical deposition of semiconductor materials (Lincot, 2005). Nowadays, the electrodeposition technique has been widely employed in the fabrication of solar cells, such as the CIGS solar cells research (Lincot, 2004) and the CdTe cells produced. Although CdS in the electrodeposition had used the thiourea as precursors (McCandless *et al.*, 1995), it was very difficult to find such a stable sulfur source in the electrodeposition CZTS.

Scragg *et al.* (2008), the Bath University in Britain employed the method of laminating and vulcanizing electrodeposition Cu/Sn/Zn to obtain the CZTS solar cells with a conversion efficiency of 0.8% (Scragg *et al.*, 2008). In 2010, by annealing for 2 hours at 575°C in an atmosphere of N<sub>2</sub> carrier gas containing S powder and 10% H<sub>2</sub>, they obtained the cells device with a conversion efficiency of 3.2% through improved technology (Scragg *et al.*, 2010).

Shinde *et al.* (2012) reported a novel chemical successive ionic layer adsorption and reaction (SILAR) technique for CZTS thin films formation by sequential reaction on solar lime glass (SLG) substrate surface. CZTS thin films were formed by sequential immersion of the substrate into the beakers containing the cationic precursor solutions of 0.1M CuSO<sub>4</sub>, 0.05M ZnSO<sub>4</sub>, and 0.05M SnSO<sub>4</sub> (1:1:1) and the anionic precursor solution of 0.2M thioacetamide. The films obtained were then annealed at 400 °C for 4h. The photoelectrochemical solar cell (PEC) cell was constructed using the annealed CZTS thin film and exhibited an efficiency of 0.12%.

### 2.2 Vacuum deposition method.

Vacuum deposition method is a physical deposition method that puts the film raw material into the vacuum chamber and heats it to high temperature to make the atoms or molecules escape from the surface then form a vapor stream entering the surface of the plated substrate; due to the low temperature of substrate, it condenses to form a solid film. Katagiri *et al.* (1997), in Nagaoka University of Technology utilized the electron beam evaporation to fabricate the Cu<sub>2</sub>ZnSnS<sub>4</sub> thin film solar cells with an efficiency of 0.66% for the first time. Later, through improving technology with employing ZnS as evaporation source, they obtained the photoelectric conversion efficiency of 2.62% Katagiri *et al.* (2001). Also through adding NaS and improving the vacuum background of annealing with a stainless steel chamber, they and obtained an efficiency of 5.45% Katagiri *et al.* (2003).

Wang *et al.* (2010) obtained the CZTS solar cell with an efficiency of 6.8% by co-evaporation, they further improved equipment and craft, employing the Cu, Zn, and Sn evaporation source of Knudsen type and Veeco S source box in metal tantalum with valves; the substrate temperature increased from 110 °C to 150 °C, and the annealing temperature increased from 540 °C to 570 °C, the annealing time was also 5 minutes. Although the film was only 600 nm, they still obtained the CZTS solar cells with an efficiency of 8.4%, which is currently the highest CZTS cells efficiency without Se (Shin *et al.*, 2011).

### 2.3 Electron beam evaporation method

Electron beam evaporation method is to employ electric field to make electron getting kinetic energy to bombard the evaporation material of anode, which can make the material vaporize to achieve evaporation coating. Nagaoka *et al.* (1996) National College of Technology Research Group, used the electron beam evaporation and curing method to fabricate the solar cells of ZnO: Al/CdS/ CZTS/Mo/SLG structure with the open circuit voltage of 400 mV, short circuit current of

6.0 mA/cm<sup>2</sup>, and fill factor of 0.277, and the conversion efficiency was only 0.66%. Yan *et al.* (2011) improved the conversion efficiency, employed Cu, Sn (or SnS<sub>2</sub>), and ZnS as vapor deposition material by electron beam evaporation method, changing the order of deposition from an evaporation to multiple cycles evaporation, using soda lime glass instead of the ordinary glass, using ZnO:Al instead of ZnO as a window layer, and finally the cells efficiency was increased to 5.45%.

Electron beam evaporation method overcomes many defects of the resistance heating evaporation, especially suitable for the production of high-melting point material and high purity thin film material. At present, preparation of the CZTS thin film with electron beam evaporation method is the most widely study in the laboratory, and the surface morphology, phase matching, and optical performance of thin film are better Yan *et al.* (2011).

#### 2.4 Magnetron sputtering method

Magnetron sputtering is that the electrons crash with Argon (Ar) atom in the electric field with ionizing abundant argon ions and electrons, and the electrons fly to the substrate. The Ar ions are accelerated in the electric field to bombard the target with sputtering a lot of target atoms, and the neutral target atoms (or molecules) are deposited on the substrate to form film.

Tanaka *et al.* (2005) for the first time used vacuum based hybrid sputtering to deposit CZTS thin films on a quartz glass substrate. Films were fabricated by the sequential deposition of metal elements and annealing in 'S' flux, varying the substrate temperature from 300 °C to 500 °C. Film thickness decreased with increase in substrate temperature. Single phase, stoichiometric CZTS film with stannite structure was obtained at 400 °C. However, composition of the thin films became Zn-poor at and above 450 °C, Resistivity, carrier concentration and Hall mobility of the films at 400 °C were 0.130 Ωcm,  $8 \times 10^{-18}$  cm<sup>-3</sup> and 6 cm<sup>2</sup> V<sup>-1</sup>s<sup>-1</sup> respectively.

Yeon *et al.* (2015) successfully prepared CZTS thin films through sulphurisation of ion beam sputtered precursors. Their results show that electrical and optical properties of the prepared films have strong dependence on atomic ratio of the constituents. By optimizing the precursor preparation conditions they obtained low resistivity of 0.1562 cm.

#### 2.5 Spray pyrolysis method

Spray pyrolysis method is to heat the surface of substrate to about 600 °C and then spray one or more metal salt solutions onto the substrate surface; high temperature will cause pyrolysis of the spray coating, which will form a coat on substrate surface. The quality and performance of thin film fabricated by spray pyrolysis relate to substrate temperature. If the substrate temperature is too high, it will be uneasy for the film to be adsorbed on the substrate; when the substrate temperature is too low, the crystallization of film will be deteriorated. According to experiment results, the CZTS thin film will have better optical property if the substrate temperature is controlled within the range of 500 °C – 650 °C in pyrolysis.

Zhang *et al.* (2010) made a reaction in CuCl<sub>2</sub>, ZnCl<sub>2</sub>, and SnCl<sub>2</sub> and vulcanized them in SC (NH<sub>2</sub>)<sub>2</sub> solution by spray pyrolysis method. The substances reacted for 1 hour at the substrate temperature of 340 °C and were annealed for 120 minutes at 550 °C. Finally, the CZTS thin films with a band gap of 1.5 eV were fabricated. The spray pyrolysis device is simple and easy to operate; the experimental procedure is simple, and no vacuum and gas protection devices are needed, so the cost is low, and the thin-film materials have good performance (Zhang *et al.*, 2010).

#### 2.6 Pulsed laser deposition method

Pulsed laser deposition method is a physical vacuum deposition process that makes the high-power pulsed laser focus on the target surface to produce high temperature and cauterization and then produce high pressure and high temperature plasma; the plasma emission expands in directional

local area and deposits the substrate to form a thin film. (Washio *et al.*, 2012) deposited CZTS thin films epitaxially on GaP substrates using pulsed laser deposition PLD. The band gap of the films was found to be 1.5 eV and films were nearly stoichiometric. (Wadia *et al.*, 2009) prepared CZTS thin films using PLD. Film was Sn-rich and the band gap was 1.5 eV. In another report, (Vigil *et al.*, 2015) prepared CZTS precursor using PLD and then annealed in N<sub>2</sub>+H<sub>2</sub>S (5 %) atmosphere.

Sugimoto *et al.* (2011) prepared polycrystalline CZTS thin films through PLD at room temperature. Study of laser incident energy revealed that structural, morphological and optical properties were improved up to incident energy of 2.5 J/cm. Shin *et al.* (2013) deposited CZTS thin films on heated Mo-coated glass substrates using PLD. Band gap of the films varied from 1.53 to 1.98 eV depending on substrate temperature. From EDAX results, all the films were Cu rich and S-deficient.

### 2.7 Screen Printing

Zhou *et al.* (2010) reported a simple and low cost screen printing approach for the preparation of CZTS absorber layers. Microparticles of CZTS prepared using wet ball milling and sintering methods, were dispersed in isopropanol. Separately, ethyl cellulose was dissolved in isopropanol. The screen printable paste was then made by mixing both solutions with small quantity of terpinol and deposited onto 'Mo' coated polyimide substrates. Band gap, sheet resistance, carrier concentration, and Hall mobility of the screen printed CZTS layers were 1.49 eV,  $2.42 \times 10^3 \Omega/\text{cm}$ ,  $3.81 \times 10^{18} \text{ cm}^{-3}$ , and  $12.61 \text{ cm}^2 \text{ V}^{-1} \text{ s}^{-1}$  respectively.

### 2.8 Chemical Bath Deposition

Chalapathi *et al.* (2015) deposited SnS and ZnS on 'Mo' coated SLG substrates through chemical bath deposition (CBD) in which 'Cu' ions were incorporated into the precursor films via ion exchange technique. These CZTS precursor films were then annealed in H<sub>2</sub>S atmosphere at 500 °C. They could produce compositionally uniform microcrystalline CZTS with kesterite structure and band gap of 1.45 eV.

### 2.9 Successive Ionic Layer Adsorption and Reaction (SILAR) Deposition

Sugimoto *et al.* (2011) reported fabrication of CZTS thin film based solar cells using similar approach. CZTS thin films were formed by sequential immersion of substrate into the solutions of cationic and anionic precursors, as deposited films were dried in oven at 60 °C for 30 min and reported an efficiency of 1.85 % on a solar cell based on CZTS prepared from SILAR technique.

Bag *et al.* (2012) reported a novel chemical successive ionic layer adsorption and reaction (SILAR) technique for CZTS thin film formation by sequential reaction on SLG substrate surface. Films were then annealed in vacuum at 400 °C. X-ray diffraction studies showed formation of kesterite structure of CZTS films.

### 2.10 Sol-Gel Deposition

Sol-gel is one of the catalysts preparation methods of CZTS thin films; it is a homogeneous process resulting in continuous transformation of a solution into hydrated solid precursor. This method has several promising advantages over the conventional techniques. It offers better control of the texture, composition, homogeneity and structural properties of the final solids.

Tanaka *et al.* (2009) reported fabrication of CZTS-based thin film solar cell using sol-gel method. They used CZTS films prepared over 'Mo' coated glass substrates by sulphurising precursors deposited by sol-gel technique as the absorber layer. Zhang *et al.* (2009) prepared CZTS films by sol-gel spin coating deposition. They avoided usual sulphurisation process. Film with a nearly stoichiometric composition was prepared at synthesizing temperature of 280 °C. Absorption coefficient and the optical energy gap of the deposited films were  $2.9 \times 10^4 \text{ cm}^{-1}$  and 1.5 eV respectively.

Wang *et al.* (2011) prepared CZTS thin films by spin-coating the sol-gel precursor followed by annealing in a nitrogen atmosphere. Band gap and absorption coefficient of the films were 1.51 eV and  $10^4 \text{ cm}^{-1}$  respectively. Zhou *et al.* (2010) deposited sol-gel processed CZTS thin films without sulphurisation. The grain size was up to 1  $\mu\text{m}$  and the Cu/(Zn+Sn) and Zn/Sn ratios were 0.93 and 1.07 respectively.

### 2.11 Hydrothermal deposition

Hydrothermal method is the methods that does not require any expensive precursors or equipment and can be readily adopted for industrial production processes. It possesses remarkable reliability and selectivity as well as high efficiency at low temperature (Habib, 2012).

Hydrothermal and solvothermal methods have been developed to prepare CZTS nanoparticles. The hydrothermal method is defined as a method that uses water as a solvent in a sealed reaction container when the temperature is raised above 100  $^{\circ}\text{C}$ , while a solvothermal method uses an organic solvent in the precursor solution (Habib, 2012).

The organic solvents such as ethylene glycol and oleylamine used in the solvothermal method are toxic and harmful to the environment. Thus, it is desirable to develop suitable hydrothermal method for fabrication of CZTS material, because of its low environmental impact (Habib, 2012).

Chopra *et al.* (2004) synthesized nanocrystalline CZTS powder through hydrothermal process using thiourea as sulphur precursor. They got kesterite CZTS of particle size 4-5 nm High temperature thermal annealing treatments are, needed for the an-deposited nanocrystal films to form large grains, which are crucial for high performance thin film solar s Based on the experience with CIGS and CIS film deposition for solar cells, films with micrometer sized grains in the absorber layer can produce cells with high power conversion efficiencies The current progresses in CZTS nanocrystal based solar cells have demonstrated that without stain growing thermal treatment process, solar cells are generally unable to generate 1% efficiency

Weber *et al.* (2010) reported that even when kesterite crystal structure nanocrystals have been formed in deposited films, thermal annealing cannot be omitted. To make CZTS thin films from the nanocrystals, CZTS nanocrystals are generally dispersed in a solvent or a mixture of solvent and binder before being subjected to film deposition. The CZTS slurry or paste with suitable rheological properties must be prepared to create a uniform layer with homogenous film thickness. The nanocrystal coatings are normally accomplished by either repeating spin coating or doctor-blading to achieve 1 to 2  $\mu\text{m}$  of film thickness, which is mostly reported as the absorber layer thickness for thin film solar cells. The as-deposited film is usually subjected to soft baking at a temperature around 300  $^{\circ}\text{C}$  followed by a high temperature annealing 500 to 580  $^{\circ}\text{C}$  for a designed duration. Although CZTE crystal ready tam the ocean amount of chalogen (sulphur in most cases)the thermal annealing process of the nanocrystal films still requires the presence of chalogen vapour Under high vacuum conditions, the CZES phase decomposes at temperature above 550  $^{\circ}\text{C}$  (Weber *et al.*, 2010). The decomposition rate largely varies depending on the temperature, total pressure of the annealing chamber, and the partial pressure of the volatile products. Therefore in order to prevent the loss of CZTS phase and the formation of undesired phases an atmospheric base pressure and a chalcogen source are normally applied in the thermal annealing process, sulphur (sulphurisation) or selenium (selenisation) is a reasonable option to prevent the decomposition of CZTS and CZTSe.

## 3.0 CHARACTERISATION

### 3.1 Visible ultraviolet spectroscopy (UV-VIS)

UV-VIS spectrophotometry is a quantitative strategy used to quantify how much a compound substance ingests light. This is finished by estimating the power of light that goes through an

example (as an element of frequency) regarding the force of light through a reference test or clear with a gadget called spectrophotometer.

UV spectrophotometer principle follows the Beer-Lambert Law. This law states that whenever a beam of monochromatic light is passed through a solution with an absorbing substance, the decreasing rate of the radiation intensity along with the thickness of the absorbing solution is actually proportional to the concentration of the solution and the incident radiation.

This law is expressed through this equation:

$$A = \log (I_0/I) = ECI \quad (1)$$

A stands for the absorbance,  $I_0$  refers to the intensity of light upon a sample cell,  $I$  refers to the intensity of light departing the sample cell,  $C$  stands for the concentration of the solute,  $L$  stands for the length of the sample cell and  $E$  refers to the molar absorptivity.

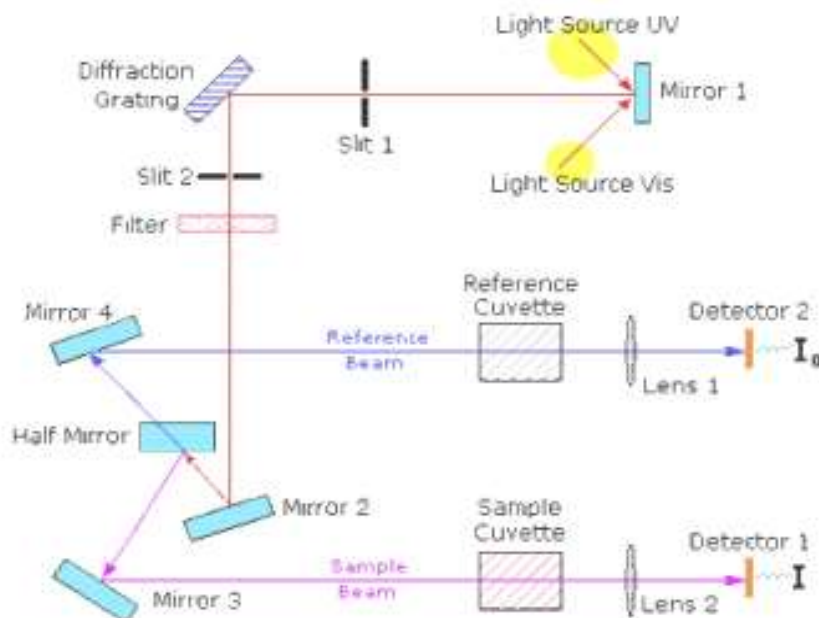


Figure 1: diagram of the components of a typical spectrophotometer (Fox, 2006).

Cho *et al.* (2013) Synthesised  $\text{Cu}_2\text{ZnSnS}_4$  thin films by a precursor solution paste, The results show that CZTS materials have low transmittance levels, indicating that the solids promote adequate absorption conditions mainly concentrated in the region of 2.0-1.54 eV, which evidence media values associated to an appropriate behavior in terms of UV absorption coefficients. The results also show a direct relationship between the synthesis temperature and the optical properties of the materials. It was observed that the energy gap decreases as the treatment temperature increases. This behavior suggests effective electronic transitions in the valence band, so that at higher temperatures a better consolidation of the Kesterite phase was achieved, decreasing the percentage of secondary phases in the CZTS materials.

Khalate *et al.* (2017), who synthesised CZTS by chemical treatment showed similar behavior and found that the optical properties of CZTS are influenced by the temperature in processes that are clearly dependent of synthesis conditions. In effect, the synthesized materials exhibit characteristic band-gap values for each system, in which the CZTS material show a remarkable result, reaching  $E_g$  values around 1.54 eV.

### 3.2 X-ray diffraction analyses

X-Ray diffraction (XRD) is an incredible procedure for assurance of precious stone design and cross section boundaries. An essential instrument for such investigation is the Bragg spectrometer as shown in fig. 3 below.

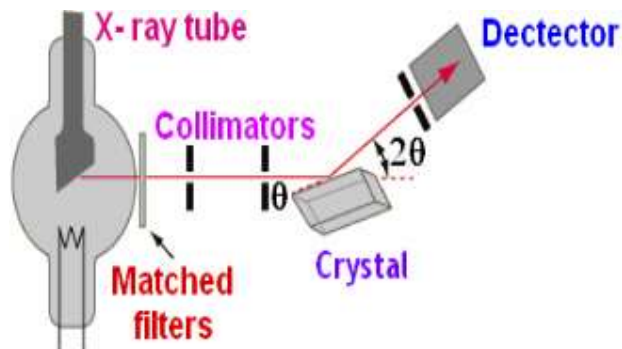


Figure 2: Schematics of X-ray diffractometer (Guinier, 1963)

Fig. 3 shows the schematics of X-ray diffractometer. Diffraction in general occurs only when the wavelength of the wave motion is of the same order of magnitude as the repeat distance between scattering centers. This condition of diffraction is nothing but Bragg's law and is given as,

$$2d \sin\theta = n\lambda \quad (2)$$

where  $d$  is inter-planer spacing,  $\theta$  is diffraction angle,  $\lambda$  is wavelength of x-ray and  $n$  is order of diffraction.

For slight movies, the powder procedure related to diffractometer is most regularly utilized. In this procedure the diffracted radiation is recognized by the counter cylinder, which moves along the rakish scope of reflections. The forces are recorded on a PC framework. The 'd' values are determined utilizing connection (2.5) for known upsides of  $\theta$ ,  $\lambda$  and  $n$ . The X-beam diffraction information in this manner got is imprinted in even structure on paper and is contrasted and Joint Committee Power Diffraction Standards (JCPDS) information to recognize the obscure material. The example utilized might be powder, single gem or slim film. The crystallite size of the stores is assessed from the full width at half greatest (FWHM) of the most exceptional diffraction line by Scherrer's equation as follows (Barrett and Massalski, 1966);

$$D = \frac{0.9\lambda}{\beta \cos\theta}$$

Where,  $D$  is crystallite size,  $\lambda$  is wavelength of X-ray used,  $\beta$  is full width at half maxima of the peak (FWHM) in radians,  $\theta$  is Bragg's angle. The X- ray diffraction data can also be used to determine the dimension of the unit cell.

According to the collection code ICDD: 00-001-1281. The presence of this phase in the solids is related to the synthesis temperature established in current work and becomes more evident in those materials that were synthesized at low temperatures. This relationship has been reported by Pinzón *et al.* (2021), observing that the intermediate phases of covallite, could be attributed to the incomplete transformation of sulphides at low temperatures. Moreover, non-stoichiometric relations of Zn, Sn and Cu can lead to formation of inhomogeneous materials Rajesh *et al.* (2013).

### 3.3 Scanning electron microscopy (SEM)

It can give significant data about the surface provisions of an item, its surface, the shape, size and plan of the particles making up the article that are lying on the outer layer of the example or have been uncovered by crushing or synthetic drawing, the components and mixtures the example is made out of and their relative proportions in regions around 1  $\mu\text{m}$  in measurement. Filtering electron microscopy (SEM) is a fundamental instrument for material portrayal particularly microstructural/morphological properties. Moreover, it can show the plan of particles in the example and their level of request. Filtering electron magnifying lens goals are at present restricted to around 25 Angstroms. The figure underneath shows a schematic outline of examining electron microscopy (Weber *et al.*, 2010).

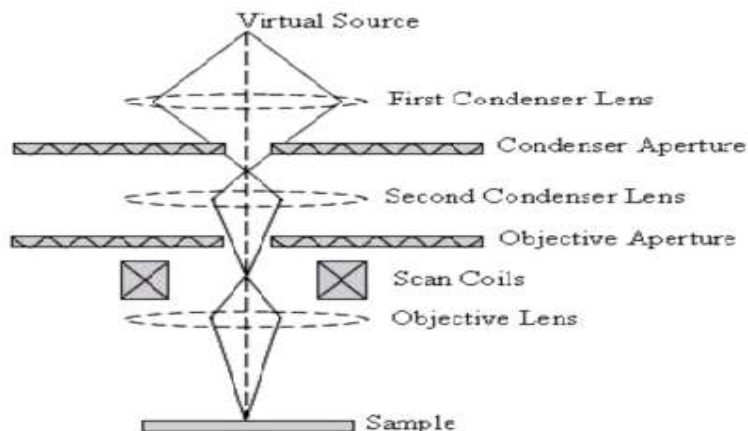


Figure 3: A schematic diagram of scanning electron microscopy

The examining electron magnifying lens produces a light emission in a vacuum. That shaft is collimated by electromagnetic condenser focal points, centered by a goal focal point, and checked across the outer layer of the example by electromagnetic redirection loops. The essential imaging strategy is by gathering optional electrons that are delivered by the example. The optional electrons are distinguished by a glimmer material that produces blazes of light from the electrons. The light glimmers are then distinguished and enhanced by a photomultiplier tube. By relating the example examine position with the subsequent sign, a picture can be shaped that is strikingly like what might be seen through an optical magnifying lens, the light and the shadowing show very normal looking surface geology (Habib, 2012).

Zhou *et al.* (2015), Reported a work via a facile liquid reflux method and the morphology of these materials was improved with increasing synthesis temperature, since the concentration of agglomerates decreased noticeably. Elemental composition analyzes performed on the CZTS samples, using X-ray dispersive energy spectroscopy (EDX), revealed that the experimental compositions differ about 1% with the theoretically calculated compositions. This difference can be caused by the tendency of zinc and tin towards the formation of sulfides at low temperatures; however, based on the properties identified up to this point and by effect of the low synthesis temperatures, it is expected that these products could be reduced in posterior thermal treatments to help to consolidate the main phase of  $\text{Cu}_2\text{ZnSnS}_4$  (Zhou *et al.*, 2015).

### 3.4 Raman spectroscopy analyses

The Raman microscopy analyzes carry out on the CZTS solids show that in addition to the characteristic signals of the CZTS material secondary phases of  $\text{Cu}_2\text{SnS}_3$ ,  $\text{Sn}_2\text{S}_3$ ,  $\text{SnS}_2$ , are observed along CZTS1-CZTS5 materials, mainly in the case of  $\text{Cu}_{2-x}\text{S}$  and  $\text{ZnS}$  phases, being clear a notable



evolution in terms of synthesis temperature Pinzón *et al.* (2017). The consolidation of a Kesterite phase is more evident in CZTS5 sample, with a strong signal around  $287\text{ cm}^{-1}$ , as indicated in Figure 4a.

The signals of magnified Raman spectrum of CZTS5 sample is shown in Figure 4b, and exhibit a more detailed evidence of secondary phases with the main peak related with the  $\text{Cu}_2\text{ZnSnS}_4$  system in the Kesterite phase. The figure shows a signal at  $338\text{ cm}^{-1}$  related to the A-symmetric vibrational mode of the Kesterite. This mode linked to the vibrations of the sulfur atoms in the crystal lattice is associated with the main signal of the CZTS molecule Pinzón *et al.* (2017). Likewise, the intense signal found at  $287\text{ cm}^{-1}$  is related to the characteristic phononic frequencies of CZTS. The signals at  $243$ ,  $255$  and  $257\text{ cm}^{-1}$  are also associated with the CZTS material.

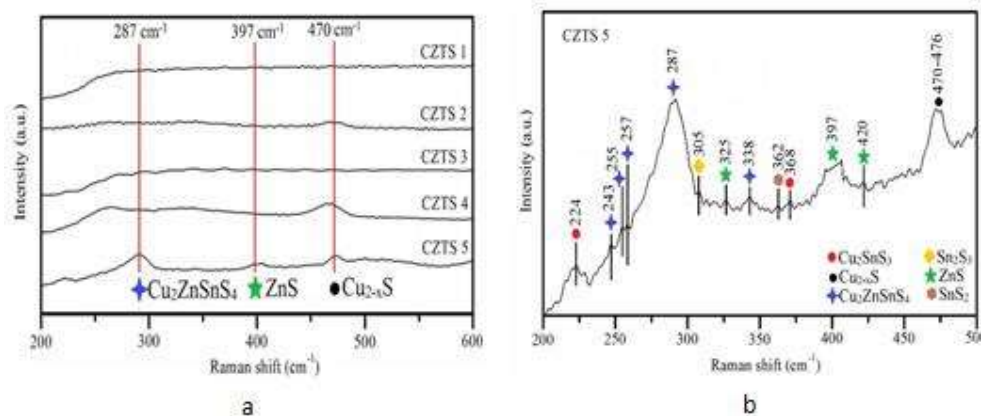


**Figure 4:** (a) Evolution of main vibrational Raman signals along CZTS1- CZTS5 samples with presence of secondary phases of ZnS and  $\text{Cu}_2\text{S}$  and (b) Raman magnified spectrum for the CZTS5 system showing the signals associated with the vibration band Pinzón *et al.* (2017).

### 3.5 Fourier transformation infrared spectroscopy (FTIR)

FTIR spectroscopy offers both qualitative and quantitative analysis for organic or inorganic samples. The basic principle of FTIR spectroscopy is to identify chemical bonds in a molecule by producing an infrared absorption spectrum. The infrared spectra then produce a profile of the sample, a distinctive molecular fingerprint as well as scan samples for different components. No two unique molecular structures can produce the same infrared spectrum, similar like a fingerprint concept. Hence, this makes infrared spectroscopy becoming very useful for many analysis categories Bag *et al.* (2012)

### 4.0 Conclusion

This review summarises recent advances of CZTS and their performance as an alternative material for costly materials like indium and gallium, this include different synthesis and characterisation method. With the further development of the preparation technology and equipment, as well as the mature theoretical research about basic features and crystallisation condition of CZTS thin film, with its environmentally friendly features, rich content in the earth crust, and good photoelectric performance, CZTS thin film will certainly become a promising photovoltaic material after CIGS thin film.

## References

- Bags, S., Gunawan, O., Gokmen, T., Zhu, Y., Todora, T.K. & Mitzi, D. B. (2012). Low band gap liquid-processed CZTS solar cell with 10.1% efficiency. *Energy Environmental Sciences*, (5): 7060-7065
- Camara, S. M., Wang, L., & Zhang, X. (2013). Easy hydrothermal preparation of Cu<sub>2</sub>ZnSnS<sub>4</sub> (CZTS) nanoparticles for solar cell application. *Nanotechnology*, 24(49), 495401.
- Chalapathi, U., Uthanna, S. & Raja, S. (2015). Growth of Cu<sub>2</sub>ZnSnS<sub>4</sub> thin films by a two stage process-Effect of incorporating of sulfur at the stage precursor. *Solar Energy materials and solar cells*, (132): 127-133
- Chen, S., Gong, X. G., Walsh, A., & Wei, S. H. (2009). Crystal and electronic band structure of Cu<sub>2</sub>ZnSnX<sub>4</sub> (X= S and Se) photovoltaic absorbers: First-principles insights. *Applied Physics Letters*, 94(4), 041903.
- Cho, J. W., Ismail, A., Park, S. J., Kim, W., Yoon, S., & Min, B. K. (2013). Synthesis of Cu<sub>2</sub>ZnSnS<sub>4</sub> thin films by a precursor solution paste for thin film solar cell applications. *ACS applied materials & interfaces*, 5(10), 4162-4165.
- Chopra, K. L, Paulson, P D & Dutta, V. (2004). Thin film solar cell: an overview Programmed Photovolt: *Research Application*, (12): 69.92
- Habib, S. L., Idris, N. A., Ladan, M. J. & Mohammed, A. G. (2012) Unlocking Nigeria's solar PV and CSP potentials for sustainable electricity development *International Journal of Scientific and Engineering Research* (5): 2010-2012
- Huang, Y., Li, G., Fan, Q., Zhang, M., Lan, Q., Fan, X. & Zhang, C. (2016). Facile solution deposition of Cu<sub>2</sub>ZnSnS<sub>4</sub> (CZTS) nano-worm films on FTO substrates and its photoelectrochemical property. *Applied Surface Science*, 364, 148-155.
- Katagiri, H., Jimbo, K., Moriya, K., & Tsuchida, K. (2003, May). Solar cell without environmental pollution by using CZTS thin film. In *3rd World Conference on Photovoltaic Energy Conversion, 2003. Proceedings of* (Vol. 3, pp. 2874-2879). IEEE.
- Katagiri, H., Nishimura, M., Onozawa, T., Maruyama, S., Fujita, M., Sega, T., & Watanabe, T. (1997, August). Rare-metal free thin film solar cell. In *Proceedings of Power Conversion Conference-PCC'97* (Vol. 2, pp. 1003-1006). IEEE.
- Katagiri, H., Saitoh, K., Washio, T., Shinohara, H., Kurumadani, T., & Miyajima, S. (2001). Development of thin film solar cell based on Cu<sub>2</sub>ZnSnS<sub>4</sub> thin films. *Solar Energy Materials and Solar Cells*, 65(1-4), 141-148.
- Khalate, S. A., Kate, R. S., Kim, J. H., Pawar, S. M., & Deokate, R. J. (2017). Effect of deposition temperature on the properties of Cu<sub>2</sub>ZnSnS<sub>4</sub> (CZTS) thin films. *Superlattices and Microstructures*, 103, 335-342.
- Khare, A., Himmetoglu, B., Johnson, M., Norris, D. J., Cococcioni, M., & Aydil, E. S. (2012). Calculation of the lattice dynamics and Raman spectra of copper zinc tin chalcogenides and comparison to experiments. *Journal of Applied Physics*, 111(8), 083707.
- Khare, A., Wills, A. W., Ammerman, L. M., Norris, D. J., & Aydil, E. S. (2011). Size control and quantum confinement in Cu<sub>2</sub>ZnSnS<sub>4</sub> nanocrystals. *Chemical communications*, 47(42), 11721-11723.
- Leitao, J. P., Santos, N. M., Fernandes, P. A., Salomé, P. M. P., Da Cunha, A. F., González, J. C., ... & Matinaga, F. M. (2011). Photoluminescence and electrical study of fluctuating potentials in Cu<sub>2</sub>ZnSnS<sub>4</sub>-based thin films. *Physical Review B*, 84(2), 024120.
- Li, J., Du, H., Yarbrough, J., Norman, A., Jones, K., Teeter, G., ... & Levi, D. (2012). Spectral optical properties of Cu<sub>2</sub>ZnSnS<sub>4</sub> thin film between 0.73 and 6.5 eV. *Optics express*, 20(102), A327-A332.
- Lincot, D. (2005). Electrodeposition of semiconductors. *Thin solid films*, 487(1-2), 40-48.
- Liu, W. C., Guo, B. L., Wu, X. S., Zhang, F. M., Mak, C. L., & Wong, K. H. (2013). Facile hydrothermal synthesis of hydrotropic Cu<sub>2</sub>ZnSnS<sub>4</sub> nanocrystal quantum dots: band-gap engineering and phonon confinement effect. *Journal of materials chemistry A*.

- Mali, S. S., Patil, B. M., Betty, C. A., Bhosale, P. N., Oh, Y. W., Jadkar, S. R., ... & Patil, P. S. (2012). Novel synthesis of kesterite Cu<sub>2</sub>ZnSnS<sub>4</sub> nanoflakes by successive ionic layer adsorption and reaction technique: characterization and application. *Electrochimica Acta*, 66, 216-221.
- McCandless, B. E., Mondal, A., & Birkmire, R. W. (1995). Galvanic deposition of cadmium sulfide thin films. *Solar energy materials and solar cells*, 36(4), 369-379.
- Pinzón, D. L., Cuaspué, J. A., Vera López, E., & Schmal, M. (2021). Hydrothermal Synthesis and Evaluation of the Cu<sub>2</sub>ZnSnS<sub>4</sub> for Photovoltaic Applications. *Materials Research*, 24.
- Pinzón, D. S., Perez, G. S., Cuaspué, J. G., & López, E. V. (2017). Synthesis and characterization of the Cu<sub>2</sub>ZnSnS<sub>4</sub> system for photovoltaic applications. In *Journal of Physics: Conference Series* (Vol. 786, No. 1, p. 012027). IOP Publishing.
- Rajesh, G., Muthukumarasamy, N., Subramaniam, E. P., Agilan, S., & Velauthapillai, D. (2013). Synthesis of Cu<sub>2</sub>ZnSnS<sub>4</sub> thin films by dip-coating method without sulphurization. *Journal of sol-gel science and technology*, 66(2), 288-292.
- Schorr, S. (2007). Structural aspects of adamantine like multinary chalcogenides. *Thin Solid Films*, 515(15), 5985-5991.
- Scragg, J. J., Dale, P. J., Peter, L. M., Zoppi, G., & Forbes, I. (2008). New routes to sustainable photovoltaics: evaluation of Cu<sub>2</sub>ZnSnS<sub>4</sub> as an alternative absorber material. *physica status solidi (b)*, 245(9), 1772-1778.
- Shin, B., Gunawa, O., Zhu, Y., Bajarczuk, N. A., Chey, S. J. & Guha, S. (2013). Thin film solar cell with 8.4 % power conversion efficiency using an earth-abundant Cu<sub>2</sub>ZnSnS<sub>4</sub> absorber. *Programmed Photovoltaic Research Application*, (21): 72-76
- Shin, B., Gunawan, O., Zhu, Y., Bojarczuk, N. A., Chey, S. J., & Guha, S. (2013). Thin film solar cell with 8.4% power conversion efficiency using an earth-abundant Cu<sub>2</sub>ZnSnS<sub>4</sub> absorber. *Progress in Photovoltaics: Research and Applications*, 21(1), 72-76.
- Shinde, N. M., Dubal, D. P., Dhawale, D. S., Lokhande, C. D., Kim, J. H., & Moon, J. H. (2012). Room temperature novel chemical synthesis of Cu<sub>2</sub>ZnSnS<sub>4</sub> (CZTS) absorbing layer for photovoltaic application. *Materials Research Bulletin*, 47(2), 302-307.
- Sugimoto, H., Hiroi, H., Sakai, N., Muraoka, S. & Katou, T. (2011). Over 8% efficiency Cu<sub>2</sub>ZnSnS<sub>4</sub> submodules with ultra-thin absorber. *IEEE photovoltaic Specialist conference 2997*
- Tanaka, K., Kasaki, D., Nishio, M. & Ogawa, H. (2009). Pneumatically sprayed CZTS films under Ar and Ar-H<sub>2</sub> atmosphere. *Journal of physics D: Applied Physics*, (47): 24:29
- Tanaka, K., Livreri, P. & Sunseri, C. (2005). A review of CZTS thin film deposition methods. *Energy Procedia*, (43): 104-109
- Vigil, G. O. Courel, M. Rodriguez, E M. Olarte D. Frutis. A M. & Sancedo, E (2015). Electrical properties of sprayed CZTS thin film and its relation with secondary phase formation and solar cell performance. *Solar Energy Materials and Solar Cells*, (132); 476-484
- Wadia, C. Alivisatos, A. P. & Kammen, D. (2009). CZTS-based solar cell from sol-gel pin Coating and its characterization. *Environment Science and Technology*, (43). 2072-2077
- Wang, K., Gunawan, O., Todorov, T., Shin, B., Chey, S. J., Bojarczuk, N. A., ... & Guha, S. (2010). Thermally evaporated Cu<sub>2</sub>ZnSnS<sub>4</sub> solar cells. *Applied Physics Letters*, 97(14), 143508.
- Wang, K., Mitzi, D. B., Barkhouse, R. & Aaron, D. (2011). Prospects and performance limitations for Cu-Zn-Sn-S-Se photovoltaic technology. *Philadelphia Transnational Royal Society*, (371): 1-22
- Washio, T., Shinj., T., Tajima, S., Fukano, T., Motohiro, T., Jumbo, K. & Katagari, H. (2015). Study of optical and structural properties of CZTS thin films grown by co-evaporation and spray pyrolysis. *Iopscience*, (65): 141-145
- Weber, R., Ishino, K., Moritake, R & Minemoto, T (2010) Improvement of CZTS thin film morphology using Cu-Zn-Sn-O precursor grown from sputtering. *Current Applied Physics*. (13) 1861-1870

- Yang, Z. (2011). Research on one-step Preparation of CZTS films and electrochemical optical properties [MS thesis]. *Dalian University of Technology*.
- Yeon, H. J., Mohauty, B. C., Denk, H.Y., Lee, S. M. & Yong, S. C. (2015). Single elementary target-sputtered  $\text{Cu}_2\text{ZnSnS}_4$  thin film solar cells. *Solar Energy Materials and solar cells*, (132): 136-141
- Zhang, S. (2010). CZTS thin film and its research progress of solar cell. *Engineering and Technology*, (8), 67-69.
- Zhang, X. G. & Shae, A. (2009). Defect physics of kesterite thin film cell absorber  $\text{Cu}_2\text{ZnSnS}_4$ . *Applied Physics Letters*, (96): 23-28
- Zhou, J., Ye, Z., Wang, Y., Yi, Q., & Wen, J. (2015). Solar cell material  $\text{Cu}_2\text{FeSnS}_4$  nanoparticles synthesized via a facile liquid reflux method. *Materials Letters*, 140, 119-122.
- Zhou, Y. L., Zhou, W. H., Du, Y. F., Li, M., & Wu, S. X. (2011). Sphere-like kesterite  $\text{Cu}_2\text{ZnSnS}_4$  nanoparticles synthesized by a facile solvothermal method. *Materials Letters*, 65(11), 1535-1537.
- Zhou, Z., Wang, Y., Xu, D. & Zhang, Y. (2010). Fabrication of  $\text{Cu}_2\text{ZnSnS}_4$  screen printed layers for solar cells. *Solar Energy Materials and Solar Cells*, (94): 2025-2042